

1 Olive oil nutritional labeling by using Vis/NIR spectroscopy and compositional 2 statistical methods

3 José A. Cayuela-Sánchez*¹, Javier Palarea-Albaladejo²

4 ¹Instituto de la Grasa, CSIC, Campus de la Universidad Pablo de Olavide, Ed. Nº 46, Crtra. De Utrera, Km 1, 41013, Seville, Spain

5 ²Biomathematics and Statistics Scotland, JCMB, The King's Buildings, EH9 3FD, Edinburgh, UK

6 *Correspondence author: jacayuela@ig.csic.es

8 Abstract

9 Food nutritional labeling is compulsory in the European Union since 13 December 2016. The
10 olive oil fatty acid composition shows high variation depending mainly on the variety. Thus,
11 olive oil nutritional labeling is problematic for the industry. Besides, the analysis of all batches
12 of olive oil using the official methods is expensive. Therefore, the olive oil industry is seriously
13 concerned about solutions for nutritional labeling. In this study, a new rapid technique to
14 measure the nutrients for the olive oil nutritional labeling, is assessed. A novel partial least
15 squares (PLS) calibration model using log-ratio coordinates has been formulated and
16 successfully tested for predicting the percentages of monounsaturated, saturated, and
17 polyunsaturated fatty acids based on visible and near infrared spectroscopy. The model
18 provided accuracy suitable for labeling, under the rules in force in the European Union. The
19 error was generally much lower than the tolerance.

20 *Industrial relevance:* The approach here proposed can be a suitable solution for olive oil
21 nutritional labeling, which is a current challenge for the olive oil industry.

22 **Keywords:** compositional data; monounsaturated fat; polyunsaturated fat; saturated fat;
23 nutritional labeling; olive oil.

24 *Abbreviations:* EVOO, extra virgin olive oils; FAME, fatty acids methyl esters; MUFA, mono-unsaturated
25 fatty acids; OO, current olive oils; PLS, partial least squares; PUFA, polyunsaturated fatty acids; SFA,
26 saturated fatty acids; TSFA, total saturated fatty acids; TUFA, total unsaturated fatty acids; Vis/NIR,
27 visible and near infrared spectroscopy; VOO, virgin olive oils.

28 1. Introduction

29 The regulation of the European Union (CE, 2011) settles the duty of food manufacturers to
30 include nutritional information in the product labels. It has been applicable since 13 December
31 2016. Olive oil results from the extraction of a substance produced by biosynthesis, in contrast

32 to what happens in foods manufactured according to a composition with several ingredients.
33 The practical challenge of nutritional labeling is different in both cases, since it depends on the
34 diversity of their nutritional features. Compulsory information includes energy value, total fat
35 contents, total saturated fatty acids (TSFA), carbohydrates, sugars, proteins and salt. As
36 voluntary nutritional information, the rule considers other nutrients' values such as mono-
37 unsaturated fatty acids (MUFA) and polyunsaturated fatty acids (PUFA), among others.
38 Regarding olive oil, the most common information included up to date in its nutritional label is
39 total fat, saturated fat, monounsaturated fat and polyunsaturated fat. The producers show
40 voluntarily these two last features. However, the olive oil industry has almost generalized their
41 inclusion in the labeling, since they characterize the product showing its nutritional
42 advantages. It is interesting also that the European Food Safety Agency issued scientific
43 opinion report on the healthy properties provided by olive oil polyphenols (EFSA, 2012).
44 Therefore, the nutritional label information on these bioactive compounds could be well
45 appreciated by the consumers.

46 In olive oil, the total fat comprises practically 100% of the product, since carbohydrates,
47 sugars, proteins and salt are absent. MUFA are those fatty acids which carbon chain have a
48 single unsaturation. The most common example of this type is oleic acid (C18:1). Its
49 unsaturation locates after the number 9 carbon, and commonly called ω -9. Oleic acid is the
50 olive oil major fatty acid, as detailed later on. Palmitoleic acid (C16:1) is the second MUFA of
51 olive oil, generally lower than 1% (García-González, Infante-Domínguez, & Aparicio, 2013^a).
52 PUFA are those fatty acids containing more than one double bond in their backbone. Good
53 human health requires diets with small quantities of these compounds, such as the essential
54 fatty acids linoleic (C18:2), ω -6, and linolenic (C18:3), this last called ω -3. Saturated fatty acids
55 (SFA) are those without any unsaturation within their chain. Olive oil includes as major SFA
56 palmitic acid (C16:0), in quantities 8-14%, stearic acid (C18:0), 3-6%, margaric acid (C17:0),
57 araquidic acid (C20:0), and behenic acid (C22:0).

58 MUFA are the most characteristic fatty acids in olive oil because of their high content of oleic
59 acid. This is helpful, since the positive effect of MUFA on cardiovascular health has been widely
60 demonstrated (Schwingshackl and Hoffmann, 2014; Hernáez et al., 2017). The olive oil fatty
61 acids show high variation depending mainly on the variety. The varieties used to produce olive
62 oil in the world are around 100, although there are more than 2000. The proportions of MUFA
63 in an olive oil depends on many agronomic conditions, the major ones being olive variety and
64 climate. Therefore, olive oils with MUFA proportions relatively small, show PUFA or SFA

65 relatively high. In addition to genetics and climate, agronomic conditions influence the
66 diversity of fatty acids. Oleic acid (18:1), which is the major fatty acid of olive oil, ranges from a
67 minimum 60.94% of Cv. Barnea in Argentina to 84.11% of Cv. Picual in New Zealand (García-
68 González, Infante-Domínguez, & Aparicio, 2013^a). At the same time, palmitic acid (16:0), the
69 major among those olive oil saturated fatty acids, ranges from 8.13% of Cv. Koroneiki in New
70 Zealand to 19.78% of Cv. Arbequina in Argentina. Diversity also exists within the product
71 manufactured by the major operators in the main producing countries, even when considering
72 some cultivars only. As an example, in the main olive oil producer, which is Spain, palmitic acid
73 ranges from 7.86% in Cv. Gordalilla to 12.55% in Cv. Negral, while oleic acid ranges from
74 66.49% in Cv. Sevillena to 81.61% in Cv. Gordalilla (García-González, Infante-Domínguez, &
75 Aparicio, 2013^a). These facts imply that generic nutritional labeling of olive oil would involve a
76 significant risk of error. Besides, the analysis of all batches of olive oil using the official
77 methods is expensive and complicated. Thus, the olive oil industry is seriously concerned
78 about the best solution for nutritional labeling. Rapid and reliable techniques to achieve this
79 purpose may be an alternative solution. Among the various non-destructive techniques that
80 have offered solutions to these needs so far, near infrared spectroscopy (NIRS) stands out for
81 its important achievements. NIR spectroscopy data analysis is based on multivariate models, in
82 which the spectral data correlate with the analyzed characteristic. Several authors (Armenta,
83 Garrigues, & De la Guardia, 2007; Bendini et al., 2007; Cayuela, Moreda & García, 2013)
84 reported the ability of NIRS to analyze the main features of olive oil quality, such as free acidity
85 or the peroxides value. In fact, a growing number of laboratories use NIRS techniques for these
86 routine analyses, although they are still a minority. The possibility of authenticating the olive
87 oil variety or geographical origin (Galtier et al., 2006, among others), as well as detecting
88 adulteration by NIRS (Azizian et al., 2015) have been also reported, in both cases through NIRS
89 analysis of their acidic composition. NIRS offers several important advantages, as it is a fast,
90 non-destructive and potentially multi-parametric method. In addition, NIRS does not need
91 solvents or reagents, therefore avoiding a significant expense and protecting the environment.

92 Chemometric methods, using traditional multivariate data analysis, are frequently applied to
93 analyze the fatty acid composition of oils and fats with diverse aims. Thus, NIR data analyses of
94 the olive oil fatty acid composition have been reported (Mailer, 2004; Mossoba et al., 2013,
95 among others). However, standard multivariate analysis techniques are formally designed for
96 ordinary unconstrained data, which take values which are directly meaningful and can be
97 compared across samples. Fatty acid profiles of plant oils are instead generally expressed as

98 relative amounts, using percentages respecting the total weight. Thus, the data information is
99 relative and there are intrinsic co-dependence relationships between components. A higher
100 percentage of one type of fatty acid will necessarily imply lower percentage of, at least, one
101 other fatty acid. Specialized theory and methods for this type of data, so-called compositional
102 data, have been developed in the statistical literature (see e.g. Aitchison, 1986, and
103 Pawlowsky-Glahn, Egozcue, and Tolosana-Delgado, 2015). Issues related to compositional
104 data have been discussed recently regarding volatile fatty acids profile of table olives (Garrido
105 et al., 2017; Garrido et al. 2018) and fatty acid composition of pork meat (Ros-Freixedes and
106 Estany, 2014). For a case in which the composition played the role of explanatory variable,
107 Palarea-Albaladejo et al. (2017) developed a compositional mixed model to explain methane
108 production from ruminal volatile fatty acids in cattle, along with other diet and animal
109 covariates. Partial least squares (PLS) analysis involving compositional data was first discussed
110 in chemometrics by Hinkle and Rayens (1995), although it was not done in terms of orthogonal
111 ILR-coordinates since this was a later development introduced by Egozcue et al. (2003). An
112 application of PLS modelling to discriminant analysis (PLS-DA), which treats the metabolomics
113 profiles as compositions via log-ratios, can be found in Kalivodová et al. (2015). However, to
114 our knowledge, there are no studies using PLS modelling under a compositional approach, to
115 predict the fat composition of vegetable oils from NIR spectroscopy through a convenient log-
116 ratio representation. Neither there are studies on the purpose of using NIRS for olive oil
117 nutritional labeling, which requires a compositional approach.

118 This study proposes a new rapid technique to measure the nutrients required for olive oil
119 nutritional labeling from Vis/NIR data. For this purpose, a novel compositional PLS calibration
120 model has been formulated, in terms of log-ratio coordinates of the percentage fatty acid
121 composition, to suitably deal with its relative scale. This model has been implemented and
122 successfully tested for estimating the percentage composition of PUFA, MUFA and TSFA. The
123 total unsaturated fatty acids (TUFA) was arithmetically determined from PUFA and MUFA.

124 **2. Material and Methods**

125 2.1. Olive Oils

126 The robustness of NIRS calibrations depends on the statistical range of the analyzed features.
127 Therefore, several sources provided olive oil samples to assure enough diversity. High quality
128 Extra Virgin Olive Oils (EVOO) from special markets contributed with 70 samples. Olive oils
129 normally found in common markets included 56 EVOO, 5 virgin olive oils (VOO) and 40 non-

130 virgin olive oils (OO). Moreover, 10 pomace olive oils were included along with 45 EVOO from
131 a collaborative industry and other 45 EVOO samples from a separate research project. These
132 were extracted at the Instituto de la Grasa (CSIC) from olives using a laboratory mill (MC2,
133 Seville, Spain) based on the Abencor system (Martínez, Muñoz, Alba, & Lanzón, 1975). In total,
134 226 samples were used.

135 2.2. Spectral Acquisition

136 The temperature of a body has an important influence on the NIR radiation it reflects and
137 absorbs, thus it is decisive in NIRS (Jiang, Xie, Peng, & Yin, 2008). Therefore, the samples were
138 taken from 4 °C storage and placed in the laboratory 18 h before processing. Before recording
139 spectra, a thermostatic bath (Nahita, London, United Kingdom) fixed at 33 °C held the 20 mL
140 sample containers for 30 min., until temperature stability was reached.

141 The spectrum of every sample was acquired with the spectrometer Labspec (Analytical
142 Spectral Devices Inc., Boulder). Labspec is equipped with three detectors. The detector for the
143 visible range (350-1000 nm) is a fixed reflective holographic diode array with a sensitivity of
144 512 pixels. A holographic fast scanner InGaAs detector cooled at -25 °C covers the wavelength
145 range of 1000-1800 nm. This coupled with a high order blocking filter runs for the 1800-2500
146 nm interval. The instrument equips internal shutters and automatic offset correction, the
147 scanning speed is 100 ms. The repeatability of the instrument, expressed as standard deviation
148 on the average absorbance of five measures of a white tile between 350 and 2500 nm, is 6.00
149 10⁻⁴ cm⁻¹ mol⁻¹. Using the Labspec, the spectra were registered by transmittance from each
150 sample of VOO directly, without any other treatment. A Hellma quartz spectrophotometric
151 cuvette with 10 mm path length held the samples while their averaged spectra were acquired.
152 The whole spectrum Vis/NIR (350–2500 nm) was registered, each spectral variable matching to
153 a 1 nm interval. Configuration for 50 spectra in continuous acquisition was used, each spectral
154 variable matching to 1 nm interval. Indico Pro software (Analytical Spectral Devices Inc.,
155 Boulder, Colorado, USA) was used for this purpose. The registering time was less than a minute
156 for each sample spectrum, all steps included.

157 2.3. Reference Analysis

158 The fatty acids compositions were analyzed by gas chromatography (GC) as fatty acid methyl
159 esters (FAME), according to the IUPAC Standard Method (IUPAC, 1987), at the Instituto de la
160 Grasa (CSIC). Briefly, 50 mg of olive oil were dissolved in 2 mL heptane and then transesterified

161 using 300 μL 2 N methanolic potassium hydroxide solution. After decanting, the supernatant
162 was collected. GC analysis was carried out using an Agilent 7697A gas chromatograph (Agilent
163 Technologies, Santa Clara) equipped with a capillary column (poly (90% biscyanopropyl–10%
164 cyanopropylphenyl) siloxane, 60 m \AA , 0.25 mm Φ , and 0.20 μm film thickness). Automatic split
165 injection and a flame ionization detector (FID) were used. The carrier gas was hydrogen at a
166 flow rate of 1 mL min^{-1} . The temperatures of the injector and detector were 225 and 250 $^{\circ}\text{C}$,
167 respectively. The oven was programmed at a temperature of 180 $^{\circ}\text{C}$ (10 min), which was then
168 increased 3 $^{\circ}\text{C min}^{-1}$ up to 220 $^{\circ}\text{C}$ (10 min). The injection volume was 1 μL . The fatty acid
169 composition was expressed as percentage of each fatty acid in total fatty acids.

170 The MUFA, PUFA, TUFA and TSFA percentages were arithmetically calculated from the
171 analyzed fatty acids values. Thus, MUFA was the sum of percentages of the fatty acids
172 palmitoleic (C16:1), heptadecenoic (C17:1), oleic (C18:1) and eicosenoic (C20:1). PUFA was the
173 sum of percentages of the fatty acids linoleic (C18:2) and linolenic (C18:3). TUFA was the sum
174 of percentages of MUFA and PUFA. TSFA was the sum of percentages of the fatty acids palmitic
175 (C16:0), stearic (C18:0), margaric (C17:0), araquidic (C20:0), and behenic (C22:0).

176 2.4. Principal Component Analysis of the Vis/NIR data

177 The absorbance data of the whole spectra were pre-treated by mean normalization and
178 Savitzsky-Golay first derivative, with polynomial order 2 and smoothing point 3. The suitability
179 of this treatment has been previously reported (Cayuela et al., 2015). The NIR and Vis/NIR
180 spectral data of the analyzed olive oil samples were reduced by principal component analysis
181 (PCA). This statistical technique projected the data onto low dimensions by computing optimal
182 linear combinations (principal components, PCs) of the measured absorbances across
183 wavelengths. In particular, the two first principal components defined dimensions accounting
184 for the highest percentage of the total variability in the original data and were used to visualize
185 the olive oil samples in an ordinary scatter plot.

186 2.5. Compositional modelling of fatty acid percentage profiles

187 Compositional data stand for all kinds of multivariate data representing parts of some whole
188 and, thus, carrying only relative information. This implies that values in each part have
189 meaning only in relation to the other parts. Percentage fatty acid compositions, consisting of
190 mutually exclusive fatty acid categories and expressed as percentages of total fatty acids,
191 correspond to this definition. Percentage compositions are formally defined on a simplex, a

192 constrained subset of the real space formed by vectors of positive values adding up to 100.
193 Compositional data bring some difficulties in relation to the most basic elements of data
194 analysis and modelling like correlations, distances, etc., which are defined according to the
195 geometry of the ordinary real space. It has been shown that the direct use of standard
196 statistical and chemometrics tools on them can introduce artifacts like negative bias in
197 correlation measures, singularity of the covariance matrix, predictions beyond the range of
198 possible values (e.g. the interval [0, 100] in our case) and results which depend on the units of
199 measurement. Obviously, these issues can potentially lead to misleading scientific conclusions.
200 A principled methodology based on using log-ratios between parts of the composition was
201 introduced in the seminal work by Aitchison (1986) and further developed thereof. A key point
202 is that all the relative information in a composition is contained in the ratios between its
203 components. Importantly, working with ratios also guarantees that results do not depend on
204 the scale of measurement of the data. Taking logs of the ratios is mathematically convenient
205 and maps the data onto the real space, where ordinary statistical methods, models and graphs
206 can be used on log-ratio coordinates (Aitchison, 1986; Van den Boogaart and Tolosana-
207 Delgado, 2013; Pawlowsky-Glahn, Egozcue, and Tolosana-Delgado, 2015).

208 2.5.1. PLS regression modeling on log-ratio coordinates

209 According to the above characterization, PLS modelling was based on log-ratio coordinates
210 involving the three fatty acid (FA) categories used as reference, MUFA, PUFA, and TSFA. In
211 particular, we employed an isometric log-ratio (ILR) representation (Egozcue et al., 2003) of
212 the 3-part FA composition, by which its information is projected onto real space by way of two
213 orthogonal coordinates as follows:

$$214 \quad \text{ILR}_1 = \sqrt{\frac{2}{3}} \ln \frac{\text{MUFA}}{\sqrt{\text{PUFA} \cdot \text{TSFA}}} \quad \text{and} \quad \text{ILR}_2 = \sqrt{\frac{1}{2}} \ln \frac{\text{PUFA}}{\text{TSFA}}. \quad [1]$$

215 Note that it is possible to define alternative ILR representations, but they all are orthogonal
216 rotations of each other and lead to the same results in terms of the original composition. An
217 ILR-coordinate roughly accounts for the relative importance of some components (in the
218 numerator of the log-ratio) with respect to others (in the denominator). The reduction from
219 three to two dimensions after the ILR transformation is coherent with the actual degrees of
220 freedom of the FA composition, we only need any two components to determine the third.
221 Multivariate PLS regression was conducted using the two ILR-coordinates of the FA
222 composition as response and the Vis/NIR spectra as predictors. Predictions obtained in ILR

223 coordinates were then transformed back into the corresponding predicted FA percentages by
224 inverse ILR transformation. After this, predicted TUFA was obtained by adding predicted
225 percentages of MUFA and PUFA.

226 A selection of best Vis/NIR spectral variables was conducted prior to multivariate PLS
227 calibration to minimize prediction error using the genetic search algorithm (Hasegawa et al.
228 1997; Mehmood et al., 2012). The PLS calibration model was fitted by the kernel algorithm to
229 predict the FA ILR-coordinates from the selected (51 out of 237) Vis/NIR spectral variables
230 (scaled by standard deviation). The optimal number of PLS latent components used (10 latent
231 components) was determined by 5-time repeated 10-fold cross validation aiming to minimize
232 the root mean square error of prediction (RMSEP) and maximize the coefficient of
233 determination (R^2) as model performance measures. The prediction performance of the final
234 joint PLS model was evaluated by RMSE and R^2 based a partition of the data into a calibration
235 data set of 75% of the data, used to tune and estimate the model as well as to assess
236 performance using 5-time repeated 10-fold cross-validation, and a test set of 25% of the data.

237 The prediction performance of the PLS model for the entire FA composition as a whole was
238 assessed by an overall R^2 , computed as the following formula:

$$239 \quad 1 - \frac{\text{totvar(ILR residuals)}}{\text{totvar(observed FA)}} \quad [2]$$

240 Where totvar, so-called total or metric variance, was obtained as the trace of the covariance
241 matrix of, respectively, the ILR residuals matrix and the observed FA data in ILR-coordinates
242 (ILR FA). Moreover, the metric standard deviation (MSD) of the ILR residuals, obtained as
243 follows:

$$244 \quad \sqrt{1/(D - 1) \cdot \text{totvar(ILR residuals)}}, \quad [3]$$

245 In this case, $D = 3$ was computed. This last statistic provided an overall dispersion measure of
246 the model residuals analogous to RMSE (Van den Boogaart and Tolosana-Delgado, 2013).
247 These statistics were obtained from calibration, cross-validation and test data. For the purpose
248 of comparison with official measurement error tolerance guidelines, analysis of the residuals
249 for each FA category separately was conducted from the cross-validation and test data sets by
250 computing the correlation between predicted and reference values and the mean percent
251 deviation of predictions with respect to the reference data. These differences were also

252 visualized for individual test samples in a scatter plot along with the official error tolerance
253 limits for reference.

254 All the data analyses and modelling described above were conducted on the R system for
255 statistical computing v3.4 (R Core Team, 2017).

256 **3. Results**

257 3.1. Olive Oil Spectra

258 The major near-infrared absorption bands of olive oil have been described by Hourant, Baeten,
259 Morales, Meurens, & Aparicio (2000). Near-infrared spectra show various overlapping bands,
260 because their first and second overtones and a combination of fundamental vibrations, mainly
261 carbon–hydrogen (Shenk, Workman, & Westerhaus, 2001). A broad absorbance band exists
262 around 1220 nm, probably due to second overtones of C–H and CH=CH– stretching vibrations
263 from oil. There is other high intensity area related to the C-H first overtone at 1700 nm (García-
264 González, Infante-Domínguez, & Aparicio, 2013^b), and a combination band at 1880–2100 nm. A
265 high intensity absorbance peak occurs about 2300 nm, caused by a combination of
266 fundamental vibrations from the C-H groups (Hourant, Baeten, Morales, Meurens, & Aparicio,
267 2000). Besides, the major visible absorption bands of olive oil were made by Moyano,
268 Meléndez, Alba, & Heredia (2008).

269 Olive oil spectra from the samples analyzed in this work, shown in Fig. 1, agree with the
270 previously indicated reports. A first minor peak occurs next to 415 nm. This area suits to the
271 wavelengths of oil absorption for dark blue colored light. It could be due mainly to carotenoids,
272 as well to pheophytin A, pheophorbide A and pyropheophytin A. A second peak is near 450
273 nm, matching to blue light absorption, which is characteristic of carotenoids. A third peak
274 appears around at 670 nm, which coincides with chlorophylls absorption (Moyano, Meléndez,
275 Alba, & Heredia, 2008). The high intensity area related to the C-H first overtone at 1700 nm
276 can be seen clearly, as well as the combination band at 1880–2100 nm and the high intensity
277 absorbance peak at 2300 nm, from the combination of fundamental vibrations of the C-H
278 groups.

279  Fig. 1

280 3.2. Fatty Acids Characterization

281 A preliminary exploration of the FA data revealed a very atypical percentage composition of
282 MUFA, PUFA, and TSFA (44.75%, 3.82%, 51.42%) of a commercial sample with registered data,
283 supposedly of olive oil and type 'acidity lower to 1%'. It was atypical particularly in relation to
284 the relative weight of TSFA (51.42%, whereas for the other samples this was around 16%), thus
285 the possibility of this corresponding to a case of fraud cannot be discarded, and it was left out
286 of the analysis.

287 Ordinary univariate descriptive statistics of the percentage MUFA, PUFA, TUFA and TSFA in the
288 olive oil samples used in this study are shown in Table 1 for reference. The TUFA ranged from
289 76.7% to 88.3%, while MUFA ranged from 57.8% to 82.4%, PUFA from 3.1% to 20.2% and TSFA
290 from 11.7% to 23.3%. The most important fatty acid category in olive oil is TUFA, with MUFA in
291 particular being the main contributor in mean (74.60%). The highest variation relative to mean
292 values was shown by PUFA ($C_v = 50.12$). Note that, given the compositional nature of the data,
293 ordinary univariate statistics of central tendency and variability for different FA categories are
294 interrelated and are not considering their particular geometry. Thus, one must interpret them
295 with caution (Pawlowsky-Glahn, Egozcue, and Tolosana-Delgado, 2015).

296 Table 1

297 3.3. PCA Analysis

298 A scatter plot based on the two first dimensions obtained from PCA analysis of the olive oil
299 spectral data is shown in Fig. 2. These two first PCs retained 77.5% of the original data
300 variability. Note that a certain 2-group structure can be appreciated along the horizontal axis
301 (first PC) in the graph. It was checked that these two groups corresponded to olive oil samples
302 separated by a MUFA content threshold at 70%. The largest group, with 180 olive oils,
303 corresponded to MUFA greater than 70%. The remaining 52 samples had MUFA less than 70%,
304 41 of them corresponding to Arbequina olive oils from super-intensive crop system obtained in
305 a research project, 4 to commercial gourmet quality EVOO, 1 to industrial EVOO, 5 to
306 commercial VOO and 1 to commercial OO samples.

307 A 95% concentration ellipse was estimated to help with the visual identification of outlying
308 spectra. The 9 samples falling beyond the boundaries of the ellipse were identified and not
309 considered for the subsequent analysis. They corresponded to 4 industrial EVOO, 1 commercial
310 EVOO, 1 commercial OO and 3 EVOO from an independent research project. Interestingly, note
311 that 7 out of these 9 outlying spectra corresponded with industrial and research samples. It is

312 frequent with this type of samples to find oils with a higher moisture content, despite having
313 been filtered as the rest ones, which differentiates their spectrum from the other samples with
314 normal moisture content. Although it is not possible to provide moisture content data, since
315 this parameter was not analyzed, we consider that this was the reason why most of these
316 samples were atypical. In the case of the two commercial samples, their spectra may be
317 defective due to methodological factors in their registering process. Hence, we eventually
318 worked with a data set consisting of 223 samples. For each one, we had the basic 3-part FA
319 composition and NIR data along 237 spectral windows. This data set was randomly partitioned
320 into calibration set (75% data, 168 samples) and test set (25%, 55 samples) for subsequent PLS
321 regression analysis.

322 Fig. 2

323 3.4. Compositional PLS model on log-ratio coordinates

324 Figure 3 displays the results from the fitted PLS model for each of the two ILR-coordinates of
325 the FA composition as detailed in Eq. [1]. Figures 3a and 3b show the respective PLS regression
326 coefficients plots using the pre-selected 51 best Vis/NIR spectral variables. Figures 3c and 3d
327 show the corresponding observed versus predicted plots. The associated model performance
328 statistics are summarized in Table 2. The most parsimonious model amongst those reaching
329 comparable highest performance following the one-standard error rule (Kuhn and Johnson,
330 2013) used 10 latent components (see Supplementary File 1). The individual ILR₁ and ILR₂
331 models provided R² equal to 0.95 and 0.90 respectively based on the calibration data (denoted
332 R²_c). The corresponding cross-validated values R²_{cv} were 0.92 and 0.83 respectively; with RPDs
333 equal to 3.53 and 2.43 respectively. The coefficients of determination from the test data set,
334 R²_v, were 0.93 and 0.86 for ILR-coordinates ILR₁ and ILR₂ respectively. Table 2 also includes the
335 calibration, cross-validation and test data based RMSE values of up to 0.10.

336 Fig. 3

337 Table 2

338 3.5. Overall model performance for predicting the FA composition

339 Predictions from the fitted PLS models on ILR-coordinates were conveniently transformed back
340 to be expressed in terms of the entire 3-part FA percentage composition. We obtained an
341 overall calibration R², which accounted for variation in the FA composition as a whole

342 explained by the model, and MSD, which accounted for dispersion in model residuals. They
343 were equal to 0.93 and 0.07 respectively (Table 2). The cross-validated and test data set
344 counterparts were 0.90 and 0.09 respectively in both cases (Table 2). Supplementary File 2
345 includes the reference and predicted values for the test data set expressed both in ILR-
346 coordinates and in terms of the entire FA percentage composition by ILR back-transformation.
347 Figure 4 illustrates the performance of the model by showing predicted (open triangles) versus
348 reference observed (open circles) FA compositions on a ternary diagram. The axes on the sides
349 of the triangle correspond with MUFA (left), PUFA (right) and TSFA (bottom) percentage
350 contents. The closer a point is to a vertex the higher the relative importance of the
351 corresponding FA in the sample. The region where the data were concentrated was zoomed in
352 for better visualization. The mean FA composition was included for reference (solid square).

353 Fig. 4

354 3.6. Assessment of model residuals by FA category

355 For each individual FA category, Table 3 provides cross-validated and test data based
356 correlation coefficients (r) between predicted and observed percentage contents and average
357 percent deviation (% deviation) of predicted with respect to observed percentage content,
358 including results for TUFA as obtained by aggregation of MUFA and PUFA. These measures
359 were useful for the assessment of the results according to current guidance for olive oil
360 nutritional labeling in the European Union, namely in relation to measurement error tolerance
361 which is set at $\pm 20\%$. The correlation coefficients for MUFA and PUFA were over 0.95 for both
362 cross-validated and test data. For TUFA and TSFA, they were around 0.9. PUFA showed the
363 highest cross-validated average percent deviation (9.61%), whereas for MUFA and TUFA it was
364 close to 1%. A comparable pattern was observed based on test data (Table 3). Figure 5
365 compares predicted and reference test values for each FA percentage individually, including
366 exact prediction line (in grey) and $\pm 20\%$ tolerance limits (in red) for reference. Predicted values
367 falling beyond the tolerance limits were obtained for TUFA and TSFA in very few isolated
368 samples. They were associated with the lowest percentage contents. Note however that,
369 according to the conceptualization of the FA percentage composition as a whole with values
370 conveying only relative information, these individual statistics and graphical representations
371 are not fully independent from one another and overall measures of performance as provided
372 in Section 3.5 would be preferable.

373 Table 3

375 **4. Discussion**

376 The assessment of the performance of the compositional PLS model based on either
377 calibration, cross-validation or test data provided R^2 s over 0.9 and RMSEs below 0.1. The
378 obtained differences between predicted and reference FA percentage compositions strongly
379 support the possibility of conducting highly accurate predictions of the FA composition of olive
380 oil samples from Vis/NIR spectroscopy data. Among them, MUFA is the most important
381 category in terms of its relative abundance and also due to its nutritional benefits for human
382 health (García-González, Infante-Domínguez, & Aparicio, 2013; Schwingshackl & Hoffmann,
383 2014).

384 The tolerances considered for the olive oil nutritional labeling have been, up to date, detailed
385 in a guidance document only (CE, 2012), which compliance is not compulsory. When the
386 nutritional component is present in less than 4g per 100g, the tolerance is ± 0.8 g, whereas
387 when it is present in more than 4g per 100g, the tolerance is $\pm 20\%$, including measurement
388 uncertainty in both cases. In this study, none of the features analyzed showed mean
389 percentage lower than 4%, thus $\pm 20\%$ tolerance is applicable. Our results show expected
390 percent deviations far within these tolerance limits, with PUFA showing the highest deviation
391 (average deviation of 9.61% from cross-validated data and of 9.59% from test data, Table 3).
392 This agrees with the higher variation coefficient of PUFA shown in Table 1. The predictions for
393 TUFA, as sum of MUFA and PUFA, also satisfied these tolerance limits.

394 **5. Conclusions**

395 The results of this study show that rapid Vis/NIR spectroscopy combined with sensible
396 chemometric modelling can be used for accurate determination of the components required
397 for olive oil nutritional labeling. Measuring the percentages of monounsaturated fatty acids,
398 polyunsaturated fatty acids, and saturated fatty acids, provided accuracy suitable for labeling
399 under the rules in force in the European Union. The data modelling conducted took into
400 account the intrinsic relative and inter-dependent nature of percentage fatty acid
401 compositions. The measured error was generally much lower than the tolerance indicated in
402 European Union guidance documentation, providing then a wide margin of safety. Thus, the
403 approach here proposed can be a suitable solution for olive oil nutritional labeling, which is a
404 current challenge for the olive oil industry.

405 **Acknowledgements**

406 J. A. Cayuela expresses gratitude to the European Regional Development Fund, aswell to the
407 Ministry of Economy and Competitiveness of Spain for funding parts of this study, which was
408 developed within the project Recupera 2020 1.4.4., and to the Spanish Council for Scientific
409 Research, for co-funding the grant 20137R065 corresponding to this project. J. Palarea-
410 Albaladejo was partly supported by the Scottish Government's Rural and Environment Science
411 and Analytical Services Division (RESAS) and by the Spanish Ministry of Economy and
412 Competitiveness under the project CODA-RETOS MTM2015-65016-C2-1(2)-R.

413 **Conflict of interests**

414 The authors declare no competing interests.

415 **References**

416 Aitchison, J. (1986). *The Statistical Analysis of Compositional Data*. Chapman and Hall, London,
417 UK.

418 Armenta, S., Garrigues, S., & De la Guardia, M. (2007). Determination of edible oil parameters
419 by near infrared spectrometry. *Analytical Chemical Acta*, 596, 330–337.
420 <http://dx.doi.org/10.1016/j.aca.2007.06.028>

421 Azizian, H., Mossoba, M. M., Fardin-Kia, A. R., Delmonte, P., Karunathilaka, S. R., & Kramer, J. K.
422 G. (2015). Novel, rapid identification, and quantification of adulterants in extra virgin olive oil
423 using near-infrared spectroscopy and chemometrics. *Lipids*, 50(7), 705–718.
424 <http://dx.doi.org/10.1007/s11745-015-4038-4>

425 Bendini, A., Cerretani, L., Di Virgilio, F., Belloni, P., Lercker, G., & Gallina-Toschi, T. (2007). In-
426 process monitoring in industrial olive mill by means of FT-NIR. *European Journal of Lipid*
427 *Science and Technology*, 109, 498–504. <http://dx.doi.org/10.1002/ejlt.200700001>

428 Cayuela J.A., Moreda W., García J.M. (2013). Rapid Determination of Olive Oil Oxidative
429 Stability and Its Major Quality Parameters Using Vis/NIR Transmittance Spectroscopy. *J. Agric.*
430 *Food Chem.* 61, 8056–8062. <http://dx.doi.org/10.1021/jf4021575>

431 Cayuela, J.A., García, J.F., Moreda, W., Pérez, M.C. 2015. Characterization of some olive oil
432 quality aspects by NIRS analysis of its fatty acids and triglycerides. Poster. 7th Symposium on
433 Recent Advances in Food Analysis. Praga, Czech Republic.

434

435 CE (2011). Regulation (EU) No 1169/2011 of the European Parliament and of the Council of 25
436 October 2011 on the provision of food information to consumers.
437 <http://eur-lex.europa.eu/legal-content/EN/TXT/PDF/?uri=CELEX:32011R1169&from=EN>. Last
438 accessed June 2017.

439 CE (2012). Orientation document for the authorities competent in the control of the
440 compliance with EU legislation on the Regulation (EU) No 1169/2011 on nutrition
441 labeling of foodstuffs.
442 [https://ec.europa.eu/food/sites/food/files/safety/docs/labelling_nutrition-vitamins_minerals-](https://ec.europa.eu/food/sites/food/files/safety/docs/labelling_nutrition-vitamins_minerals-guidance_tolerances_1212_en.pdf)
443 [guidance_tolerances_1212_en.pdf](https://ec.europa.eu/food/sites/food/files/safety/docs/labelling_nutrition-vitamins_minerals-guidance_tolerances_1212_en.pdf). Last accessed June 2017.

444 EFSA (2012). Scientific Opinion on the substantiation of a health claim related to polyphenols
445 in olive and maintenance of normal blood HDL-cholesterol concentrations pursuant to Article
446 13(1) of Regulation (EC) No 1924/2006. *EFSA Journal* 10(8), 2848.

447 Egozcue, J. J., Pawlowsky-Glahn, V., Mateu-Figueras, G., Barceló-Vidal, C. (2003). Isometric Log-
448 ratio Transformations for Compositional Data Analysis. *Mathematical Geology*, 35(3), 279-300.

449 Galtier, O.; Dupuy, N.; Le Dreau, Y.; Ollivier, D.; Pinatec, C.; Kister, J.; Artaud, J. (2006).
450 Geographic origins and compositions of virgin olive oils determined by chemometric analysis
451 of NIR spectra. *Analytical Chemical Acta*, 595, 136-144.
452 <https://doi.org/10.1016/j.aca.2007.02.033>

453 García-González, D. L., Infante-Domínguez, C., Aparicio, R. (2013^a). Tables of Olive Oil Chemical
454 Data. In R. Aparicio, & J. Harwood (Eds.), *Handbook of olive oil: Analysis and properties* (pp.
455 739-768). New York: Springer.

456 Garrido-Fernández, A., Montañó, A., Sánchez-Gómez, A. H., Cortés-Delgado, A., López-López,
457 A. (2017). Volatile profiles of green Spanish-style table olives: Application of compositional
458 data analysis for the segregation of their cultivars and production areas. *Talanta*, 169, 77-84.
459 <http://dx.doi.org/10.1016/j.talanta.2017.03.066>

460 Garrido-Fernández, A., Cortés-Delgado, A., López-López, A. (2018). Tentative application of
461 compositional data analysis to the fatty acid profiles of green Spanish-style Gordal table olives.
462 *Food Chemistry*, 241, 14-22. <http://dx.doi.org/10.1016/j.foodchem.2017.08.064>

463 Hasegawa, Y. Miyashita, K. Funatsu. (1997). GA strategy for variable selection in QSAR studies:
464 GA-based PLS analysis of calcium channel antagonists. *Journal of Chemical Information and*
465 *Computer Sciences*, 37, 306-310. <http://dx.doi.org/10.1021/ci960047x>

466 Hernandez, A., Casta˜ner, O., Goday, A., Ros, E., Pinto, X., Estruch, R., Salas-Salvado, J., Corella, D.,
467 Aros, F., Serra-Majem, L., Martinez-Gonzalez, M. A., Fiol, M., Lapetra, J., De la Torre, R., Lopez-
468 Sabater, M.C., Fito, M. (2017). The Mediterranean Diet decreases LDL atherogenicity in high
469 cardiovascular risk individuals: a randomized controlled trial. *Molecular Nutrition & Food*
470 *Research*, 61(9), 1601015, 9 pp. <http://dx.doi.org/10.1002/mnfr.201601015>

471 Hinkle, J., W. Rayens. (1995). Partial least squares and compositional data: problems and
472 alternatives. *Chemometrics and Intelligent Laboratory Systems*, 20, 159-172.
473 [https://doi.org/10.1016/0169-7439\(95\)00062-3](https://doi.org/10.1016/0169-7439(95)00062-3)

474 Hourant, P., Baeten, V., Morales, M. T., Meurens, M., & Aparicio, R. (2000). Oil and fat
475 classification by selected bands of near-infrared spectroscopy. *Applied Spectroscopy*, 54,
476 1168–1174.

477 IUPAC (1987). Standard Method 2.302. Standard methods for the analysis of oils, fats and
478 derivatives. Determination of FAMES by capillary GC. Blackwell Scientific: Oxford, Great Britain.

479 Jiang, H.Y., Xie, L.J., Peng, Y.S., Yin, Y.B. (2008). Study on the influence of temperature on near
480 infrared spectra. *Guang Pu Xue Yu Guang Pu Fen Xi*, 28(7), 1510-1513.

481 Kalivodova, A., Hron, K., Filzmoser, P., Najdekr, L., Janeckova, H., Adam, T. (2015). PLS-DA for
482 compositional data with application to metabolomics. *Journal of Chemometrics*, 29, 21–28.
483 <http://dx.doi.org/10.1002/cem.2657>

484 Kuhn, M., Johnson, K. (2013). *Applied Predictive Modelling*. New York, Springer.
485 <http://dx.doi.org/10.1007/978-1-4614-6849-3>

486 Mailer, R. J. (2004). Rapid evaluation of olive oil quality by NIR reflectance spectroscopy.
487 *Journal of the American Oil Chemists Society*, 81, 823-827.

488 Martinez, J.M., Mu˜oz, E., Alba, J., Lanzon, A. (1975). Report on the use of the Abencor olive oil
489 yields analyser. *Grasas y Aceites*, 26, 379-385.

490 Mehmood, K.H. Liland, L. Snipen, S. Sæbø. (2012). A review of variable selection methods in
491 Partial Least Squares Regression. *Chemometrics and Intelligent Laboratory Systems*, 118, 62-
492 69. <https://dx.doi.org/10.1016/j.chemolab.2012.07.010>

493 Mossoba, M. M.; Azizian, H.; Tyburczy, C.; Kramer, J. K. G.; Delmonte, P.; Kia, A. R. F.; Rader, J.
494 I. (2013). Rapid FT-NIR Analysis of Edible Oils for Total SFA, MUFA, PUFA, and Trans FA with
495 Comparison to GC. *Journal of the American Oils Chemists Society* 90(6), 757-770.
496 <https://dx.doi.org/10.1007/s11746-013-2234-z>

497 Moyano, M. J., Meléndez, A. J.; Alba, J., & Heredia, F. J. (2008). A comprehensive study on the
498 colour of virgin olive oils and its relationship with their chlorophylls and carotenoids indexes
499 (I): CIEXYZ non-uniform colour space. *Food Research International*, 41, 505–512.
500 <https://doi.org/10.1016/j.foodres.2008.03.007>

501 Palarea-Albaladejo, J., Rooke, J. A., Nevison, I. M., Dewhurst, R. J. (2017). Compositional mixed
502 modeling of methane emissions and ruminal volatile fatty acids from individual cattle and
503 multiple experiments. *Journal of Animal Science*, 95, 2467-2480.
504 <https://doi.org/10.2527/jas2016.1339>

505 Pawlowsky-Glahn, V., Egozcue, J. J., Tolosana-Delgado, R. (2015). *Modeling and Analysis of*
506 *Compositional Data*. Wiley & Sons, Chichester, UK.
507 <https://doi.org/10.1002/9781119003144.ch1>

508 R Core Team. (2017). R: A Language and Environment for Statistical Computing. R Foundation
509 for Statistical Computing, Vienna, Austria. <https://www.R-project.org>

510 Ros-Freixedes, R., and J. Estany. (2014). On the compositional analysis of fatty acids in pork.
511 *The Journal of Agricultural, Biological and Environmental Statistics*, 19, 136–155.
512 <https://doi.org/10.1007/s13253-013-0162-x>

513 Schwingshackl, L., Hoffmann, G. (2014). Monounsaturated fatty acids, olive oil and health
514 status: a systematic review and meta-analysis of cohort studies. *Lipids in Health and Disease*,
515 13, 154. <https://doi.org/10.1186/1476-511X-13-154>

516 Shenk, J. S.; Workman, J. J.; Westerhaus, M. O. (2001). Application of NIR spectroscopy to
517 agricultural products. In: D. A. Burns, and C. W. Ciurcak (Eds.), *Handbook of Near Infrared*
518 *Analysis*, 2nd Edition (pp. 419–474). New York: Marcel Dekker.

519 Van den Boogaart, K. G.; Tolosana-Delgado, R. (2013). *Analyzing Compositional Data with R*.
520 Springer, Heidelberg, Germany. <https://doi.org/10.1007/978-3-642-36809-7>

521 **Figure captions**

522 Figure 1. Vis/NIR spectra of the olive oil samples analyzed.

523 Figure 2. Principal component analysis of olive oil Vis/NIR spectral data (first PC on the
524 horizontal axis and second PC on the vertical axis).

525 Figure 3. Compositional PLS model results: PLS regression coefficient estimates of individual
526 models for the first (a) and second (b) ILR-coordinates of the FA composition and
527 corresponding predicted versus observed plots (c) and (d) respectively.

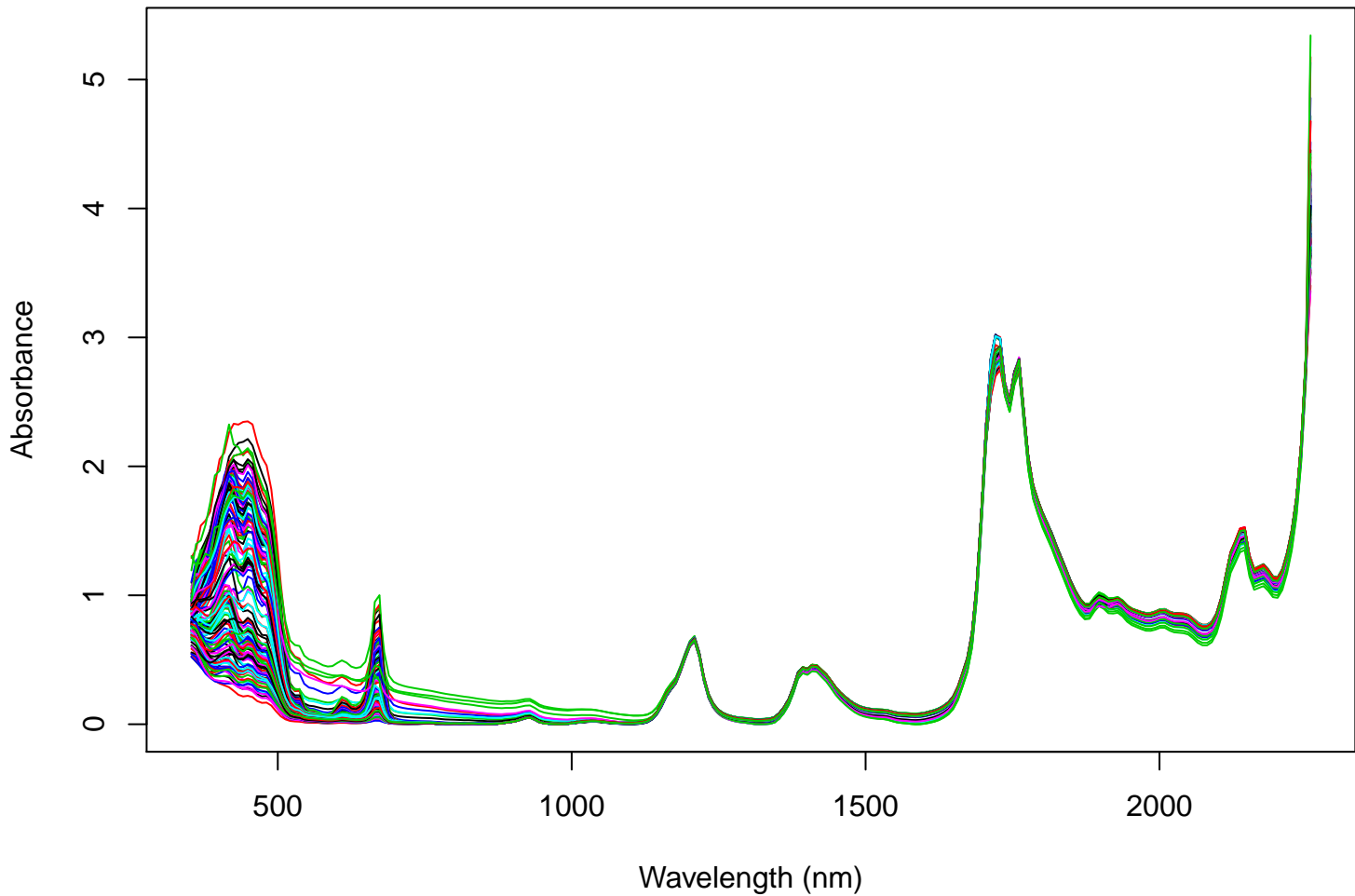
528 Figure 4. Ternary plot of the predicted and observed FA percentage compositions from the
529 fitted compositional PLS model.

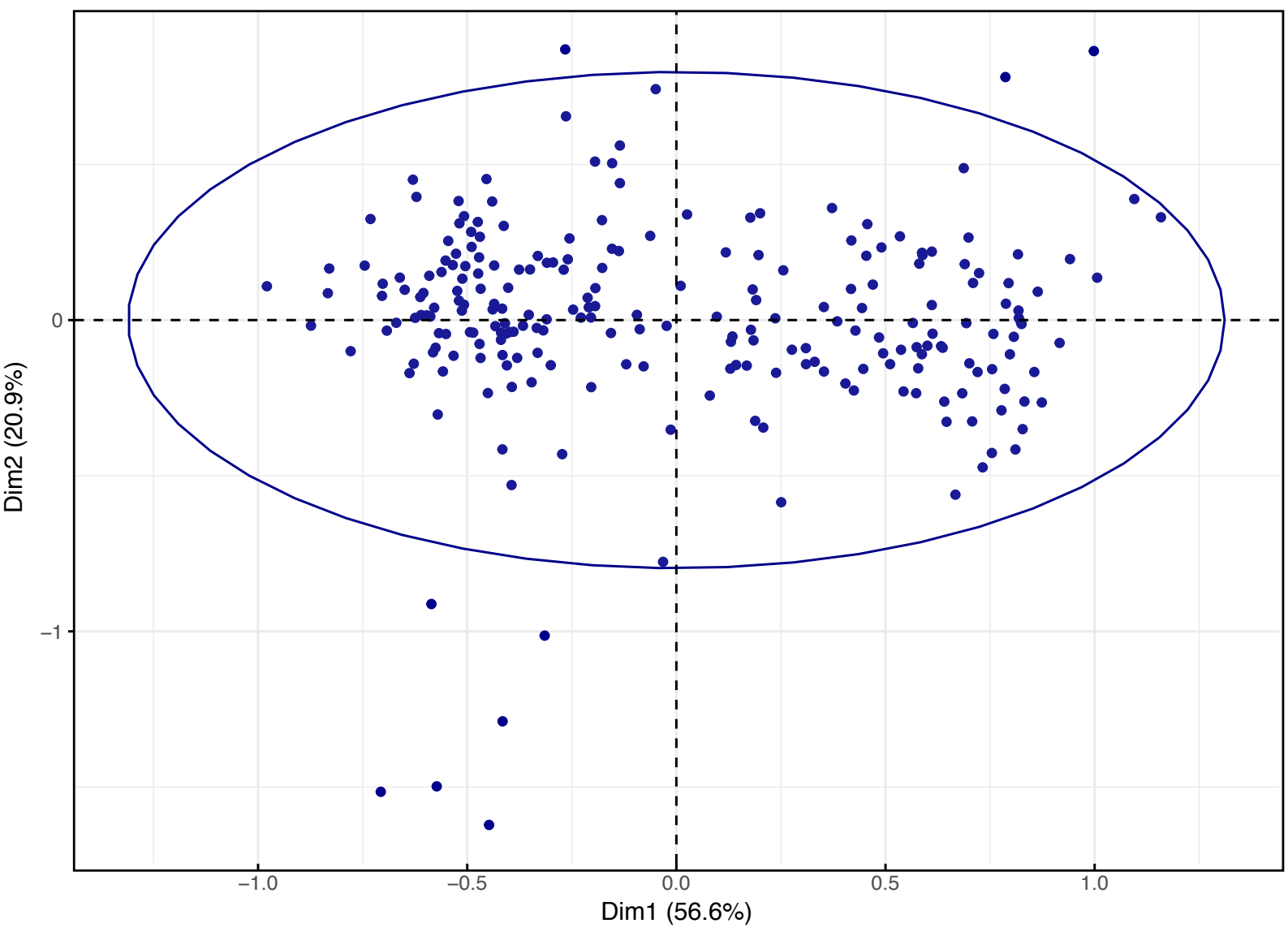
530 Figure 5. Predicted and observed percentage contents for individual FA categories based on
531 test data (including $\pm 20\%$ tolerance limits according to European Union guidance).

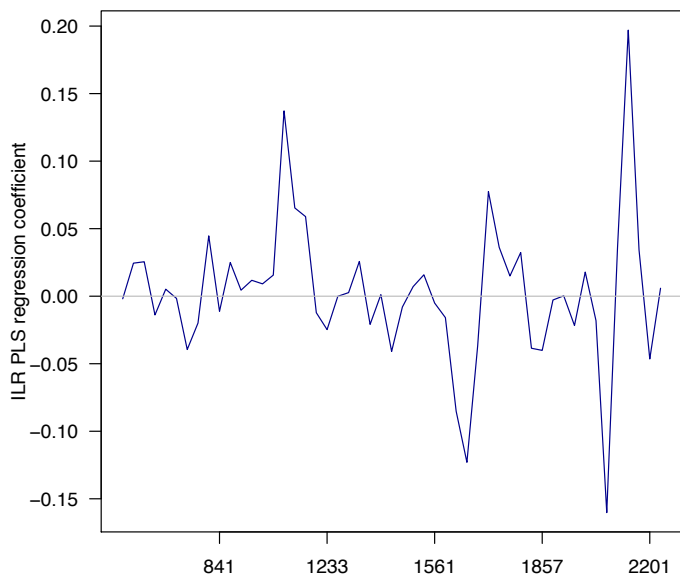
532

533

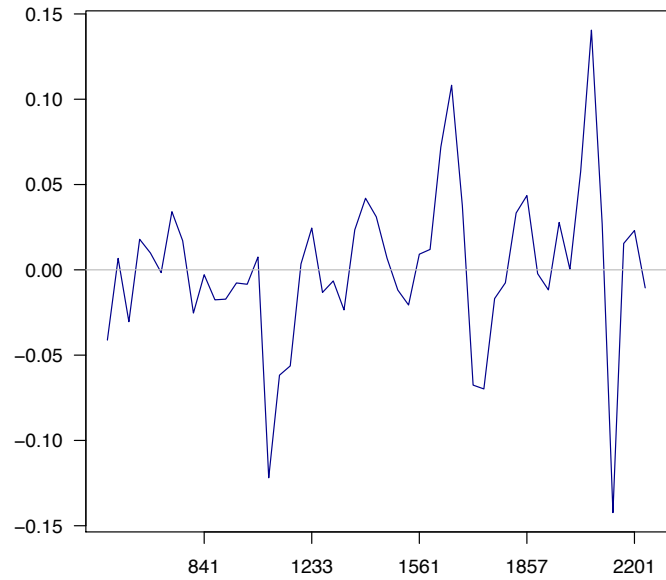
534



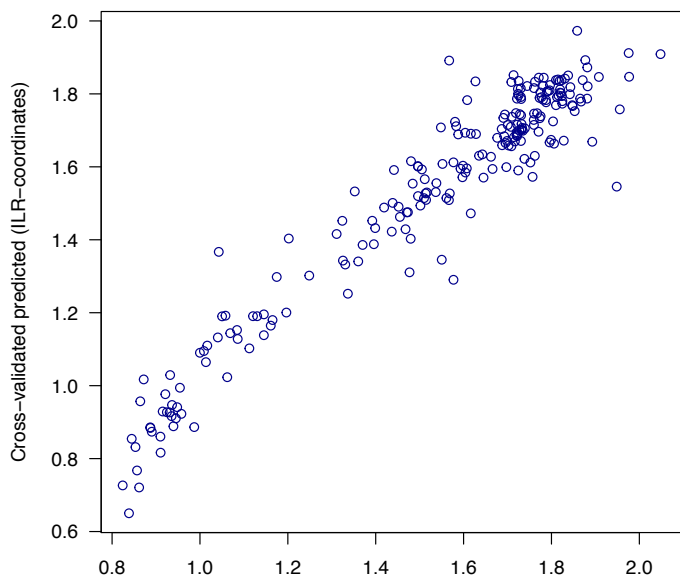


FA ILR₁

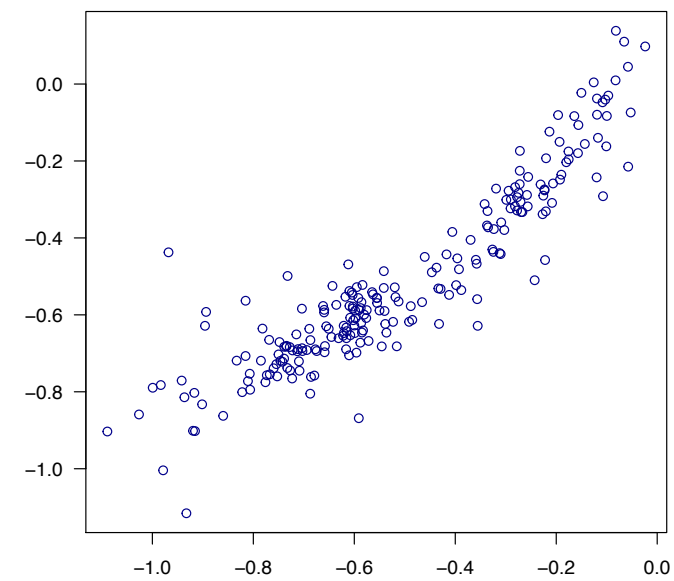
(a)

FA ILR₂

(b)



(c)



(d)

%PUFA

FA composition

- Mean
- Observed
- △ Predicted

